Synthesis, characterization, and photophysical properties of cyclometalated N-Heterocyclic carbene Platinum(II) complexes

Francesco Mastrocinque [a], Craig M. Anderson [a, *], Adel M. Elkafas [a], Isabel V. Ballard [a], Joseph M. Tanski [b]

[a] Department of Chemistry, Bard College, Annandale-on-Hudson, NY, 12504, USA
[b] Department of Chemistry, Vassar College, Poughkeepsie, NY, 12604, USA

ARTICLE INFO

ABSTRACT

Thiophene and benzothiophene ligands containing N-heterocyclic carbene (NHC) moieties were used to synthesize five and six-membered Pt(II) metallacycles. Ligand scaffolding was synthesized using two methods. The ligands were synthesized using a coupling reaction, utilizing Cu_2O as the catalyst or were synthesized using a nucleophilic substitution reaction. The ligands were then metalated by chelate-assisted C—H activation. The synthesis, characterization, reactivity, and photophysical properties of these NHC-functionalized, cyclometalated products are reported.

© 2018 Published by Elsevier B.V.

1. Introduction

N-heterocyclic carbenes (NHCs) have become a prominent ancillary ligand in organometallic chemistry. Their strong σ-donation and reluctant π-backbonding allows NHCs to form stable bonds with transition metals [1–4]. Recently, platinum(II) NHC complexes have found applications in photovoltaics, medicine, and catalysis [5–7].

Transition-metal complexes displaying long lifetimes are of interest for phosphorescent organic light emitting diodes (PHOLEDs), substrate detectors, and biological labeling agents [8–10]. Transition-metal complexes are of great importance to the development of highly efficient photoluminescence materials due to their strong spin-orbit coupling, allowing for intersystem crossing (ISC) [11]. NHCs have been shown to coordinate to a variety of transition metals as bidentate ligands [12–14]. In addition, cyclometalated platinum(II) NHC complexes bearing acetylacetonate (acac) auxiliary ligands have previously demonstrated efficient photoluminescence [15–17] while the π-extension of the NHC ligand backbone can allow for energy level fine-tuning [18].

Thiophene ligands have been previously explored for applications in dye-sensitized solar cells (DSSC), nonlinear optics, and photodetectors [19–21]. In addition to their photophysical implications, synthesis of thiophene ligands and subsequent metalation is well established [22–24]. Benzothiophenes are structures that are part of pharmaceuticals and biologically active species [25,26]. Different ring sizes have also been of interest in tuning the photophysical properties and reactivity of cyclometalated platinum complexes [27–30]. Furthermore, the regioselectivity of cyclometalated complexes by C—H activation is of interest due to the possible formation of different metallacycle sizes [31–33]. The photophysical properties, regioselectivity, and reactivity of five and six-membered cyclometalated platinum(II) complexes containing bidentate NHC ligands are reported.

---

* Corresponding author.
   E-mail address: canderso@bard.edu (C.M. Anderson).
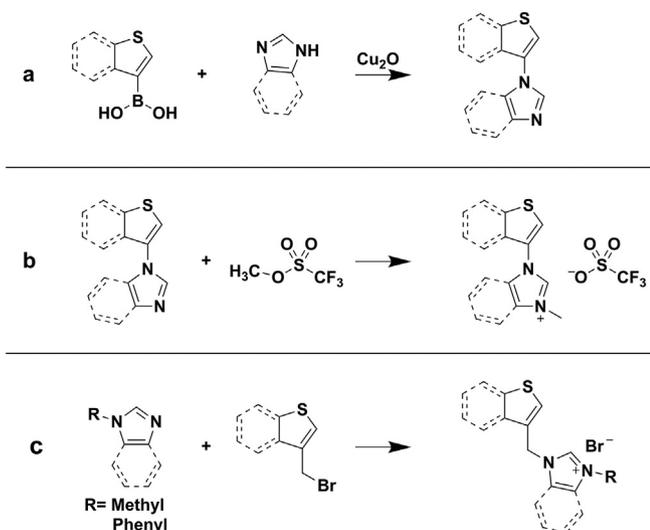
2. Results and discussion

2.1. Synthesis and characterization

The eight ligands synthesized for this work can be categorized into two groups. The first group has a direct C–N bond between ring systems that ultimately generate five-membered platinacycles and the second group has a methylene spacer between the ring systems that ultimately generate six-membered platinacycles (Chart 1). Ring coupling was performed utilizing a previously described procedure [34], similar to an Ullmann coupling reaction. The coupling reaction was facilitated by Cu_2O and used to synthesize a flat, aromatic scaffolding (Scheme 1a). The coupled products were subsequently subjected to nucleophilic substitution reactions to form the imidazolium precursors (Scheme 1).
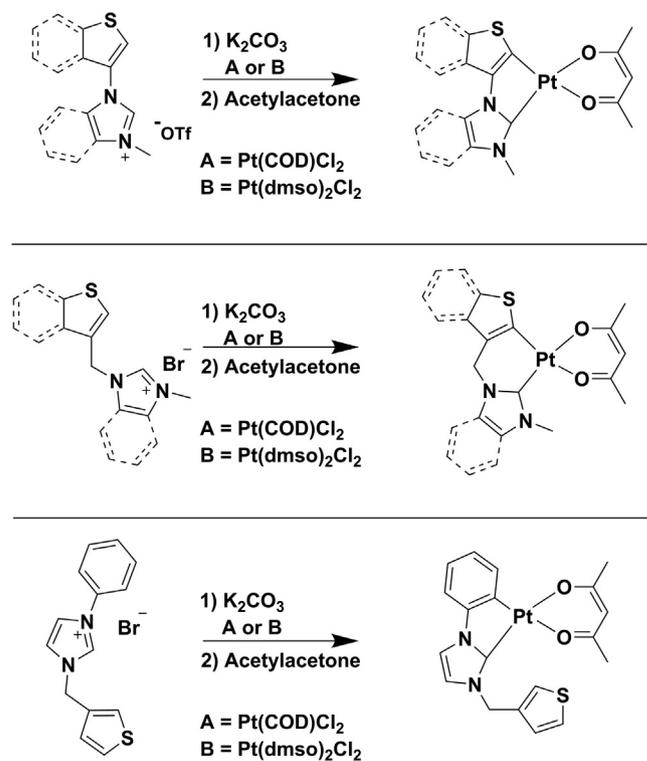
Cyclometalated complexes were synthesized using a two-step, one-pot procedure (Scheme 2). The bidentate NHC and acetylacetonate (acac) ligands were generated in situ with the use of K_2CO_3 as a mild base.

Dichloro(1,5-cyclooctadiene)platinum(II), Pt(COD)Cl_2, and dichlorobis(dimethyl sulfoxide)platinum(II), Pt(dmso)$_2Cl_2$, were used as platinum precursors [35,36]. All metalated complexes were purified by flash chromatography using methylene chloride and hexane as eluent. Complexes were obtained in acceptable yields (21–54%).

The metalated products were characterized by NMR spectroscopy, HRMS, and several samples (Pt1, Pt3, Pt4, Pt7, and Pt8) by X-ray diffraction (XRD) techniques. Most metalated complexes could be fully elucidated using ^1H and COSY NMR spectra, however overlap of the numerous aromatic resonances did not permit complete assignments of all downfield resonances for all complexes. Methyl groups located on the acac ligand, the methylene group on the six-membered metallacycles, and the methyl group on the methyl-functionalized NHC ligands provided excellent markers and were tabulated for all compounds. Using these distinguishable resonances, coupling to neighboring protons observed in the COSY and NOESY spectra allowed for additional assignments in the spectrum. The successful coordination of the acac ligand was verified by the presence of the methine proton resonance signal in the ^1H NMR.

Scheme 2. Synthesis of metalated complexes using two-step, one-pot synthetic procedure.

X-ray diffraction methods confirmed the structures of both five and six-membered metallacycles. The NMR spectra for Pt1, Pt3, Pt4, Pt7, and Pt8, in conjunction with XRD results, allowed these complexes to be used as references for elucidating the NMR assignments and structures of the other metallacycles.

The regioselective formation of Pt7 is of particular interest to us. The presence of two aromatic R groups located on the NHC allow two distinct intramolecular C–H activation pathways to potentially occur, forming either a five or a six-membered metallacycle. However, characterization by NMR (Fig. 1) and XRD confirm the formation of only the five-membered cyclometalated product, instead of the six-membered metallacycle, that without incorporation of the thiophene. The proton and COSY NMR spectra of Pt7 indicate a singlet located at a shift of 7.30 ppm that couples with a
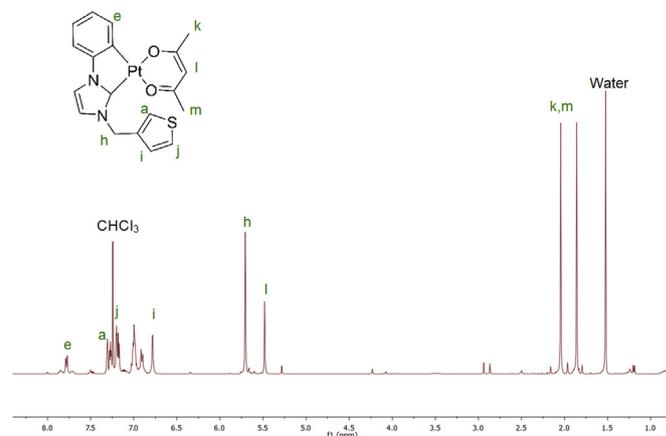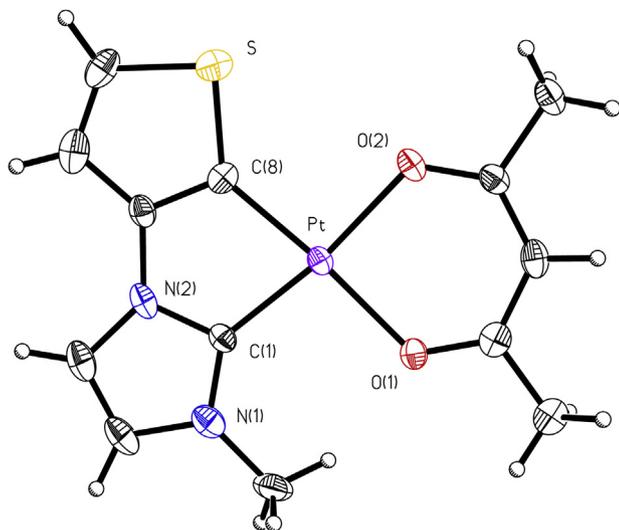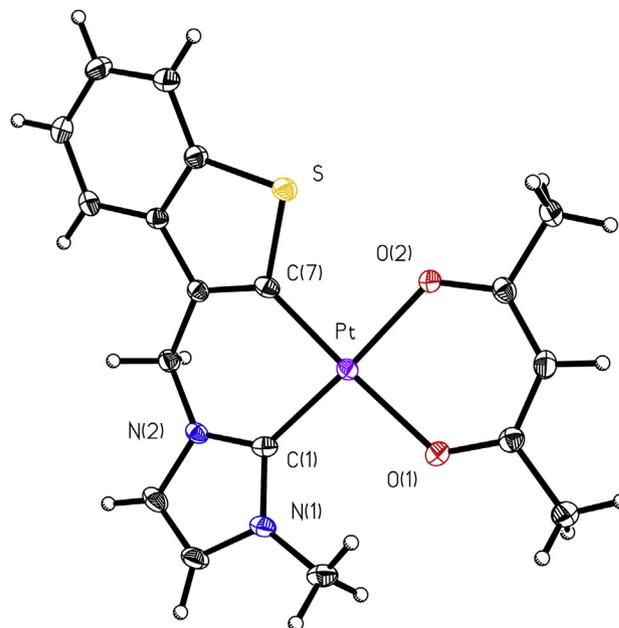

Scheme 1. Depiction of N-arylation reaction (a) and subsequent nucleophilic substitution reaction (b) and (c). Pre-functionalized (benz)imidazole complexes and an alkyl halide were also used to form the imidazolium salt precursor.

Fig. 1. ^1H NMR spectrum of Pt7.

Fig. 2. ORTEP of Compound **Pt1** (50% probability thermal ellipsoids). Selected bonds lengths (Å) and angles (°): Pt–C(1): 1.965(5); Pt–C(8): 1.981(5); Pt–O(2): 2.049(4); Pt–O(1): 2.071(4); C(1)–Pt–C(8): 79.0(2); C(1)–Pt–O(2): 172.05(18); C(8)–Pt–O(2): 93.02(19); C(1)–Pt–O(1): 96.28(18); C(8)–Pt–O(1): 175.13(17); O(2)–Pt–O(1): 91.64(14).

signal at 5.70 ppm, indicating coupling between the methylene "spacer" protons and the C(2) position on the thiophene moiety. In addition, the presence of a broad doublet with satellites located furthest downfield on the ¹H NMR is consistent with previous literature describing metallacycles containing a phenyl moiety [37].

2.2. Photophysical results

All metalated complexes were characterized by UV-Vis absorbance and emission spectroscopy in order to investigate their photophysical properties. All complexes studied in this work have distinct absorption bands in the region of 325—405 nm with extinction coefficients on the order of 10^3 or 10^4. The large Stokes shifts (Table 1) found in these complexes are in good agreement with previous compounds for assigning these bands a ^{3}MLCT [38].

Fig. 3. ORTEP of Compound **Pt3** (50% probability thermal ellipsoids). Selected bonds lengths (Å) and angles (°): Pt–C(1): 1.9526(17); Pt–C(12): 1.9673(16); Pt–O(2): 2.0364(13); Pt–O(1): 2.0630(12); C(1)–Pt–C(12): 79.20(7); C(1)–Pt–O(2): 171.18(6); C(12)–Pt–O(2): 92.31(6); C(1)–Pt–O(1): 97.47(6); C(12)–Pt–O(1): 175.74(6); O(2)–Pt–O(1): 90.90(5).
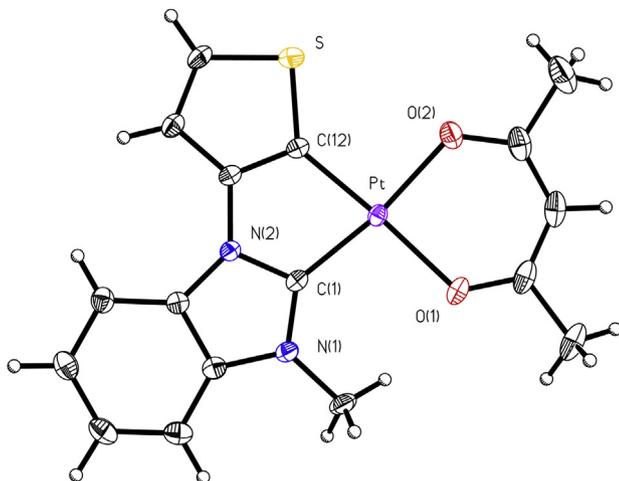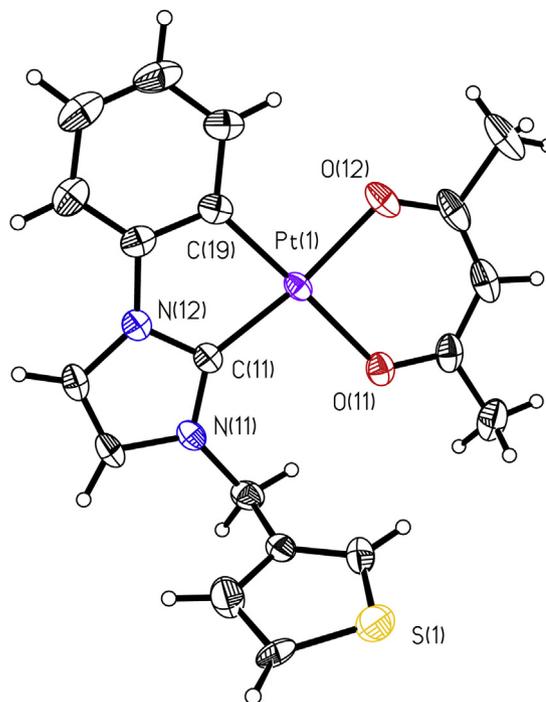

Fig. 4. ORTEP of Compound **Pt4** (50% probability thermal ellipsoids). Selected bonds lengths (Å) and angles (°): Pt–C(1): 1.966(3); Pt–C(7): 1.969(3); Pt–O(1): 2.054(2); Pt–O(2): 2.085(2); C(1)–Pt–C(7): 88.15(12); C(1)–Pt–O(1): 176.39(11); C(7)–Pt–O(1): 88.24(10); C(1)–Pt–O(2): 94.30(11); C(7)–Pt–O(2): 177.40(11); O(2)–Pt–O(1): 89.32(9).

All complexes are either blue, blue-green, or green emitters with emission bands within the 430—530 nm region. For the six-membered metallacycles, the benzothiophene-containing complexes displayed a lower magnitude red-shifted emission band

Fig. 5. ORTEP of Compound **Pt7** (50% probability thermal ellipsoids). Selected bonds lengths (Å) and angles (°): Pt–C(11): 1.944(3); Pt–C(19): 1.987(3); Pt–O(12): 2.048(2); Pt–O(11): 2.086(2); C(11)–Pt–C(19): 80.09(12); C(11)–Pt–O(12): 171.62(10); C(19)–Pt–O(12): 91.71(11); C(11)–Pt–O(11): 97.85(10); C(19)–Pt–O(11): 176.51(9); O(12)–Pt–O(11): 90.25(9).

Table 1
Tabulated emissive properties of all complexes at room temperature ($\lambda_{ex} = 365$ nm).

Class	Complex	λ at Max Intensity (nm) [$\lambda_{ex} = 365$ nm]	Stoke Shift (nm from 365 nm)	Lifetime (ns)
Class A: Imidazole-2-ylidene Metalated Products	**Pt1**	508	143	241
	Pt4	488	123	766
	Pt7	527	162	959
	Pt8	525	160	528
Class B: Benzimidazol-2-ylidene Metalated Products	**Pt2**	534; 567	169; 202	989
	Pt3	505; 527	140; 162	743
	Pt5	467; 495	102; 130	447
	Pt6	459; 529	94; 164	350

compared to their thiophene-containing analogues. The opposite effect is noted in the five-membered metallacycles, where the benzothiophene-containing analogues displayed a greater red-shifted emission band compared to their thiophene-containing analogues.

The cyclometalated imidazole-2-ylidene complexes (Chart 1, Class A) display broad emission bands (Fig. 7). **Pt4** is the only one of these four in Class A that is a true blue emitter ($\lambda_{max} = 488$ nm). All other cyclometalated imidazole-2-ylidene complexes (Class A) are green or blue-green emitters. **Pt4** and **Pt1** possess shoulders located at higher energies than their maximum emission peak (λ_{max}).

The cyclometalated benzimidazol-2-ylidene complexes (Chart 1, Class B) display different photophysical properties than their cyclometalated imidazole-2-ylidene (Class A) counterparts.

Two emission bands are observed for each cyclometalated benzimidazol-2-ylidene complex (Fig. 8). This may be due to excimer formation, which has been observed for platinum(II) complexes bearing NHCs with extended π-systems [39]. **Pt5** is the only true blue emitter in the cyclometalated benzimidazol-2-ylidene class of complexes (Chart 1, Class B) studied. The rest of this class are all blue-green or green emitters. It is interesting to note that the cyclometalated benzimidazol-2-ylidene complexes containing benzothiophene moieties (**Pt5** and **Pt2**) exhibit shoulders at lower energies than their λ_{max}. However, the cyclometalated

benzimidazol-2-ylidene complexes containing thiophene moieties (**Pt6** and **Pt3**) exhibit shoulders at higher energies than their λ_{max}.

The excited state lifetimes for all metalated complexes were measured at $\lambda_{ex} = 365$ nm. The lifetimes of the excited states for all complexes were in the 201–989 ns range (Table 1), which is consistent with emission from a ^{3}MLCT excited state [40].

2.3. Reactivity of complexes with MeI

In order to determine the reactivity of the complexes with respect to the fundamental organometallic reactions, oxidative addition and reductive elimination, the complexes were allowed to react with methyl iodide (MeI) (Scheme 3). Upon addition of 100 equivalents of MeI to a solution of the cyclometalated products, new Pt(IV) species were formed by *trans* oxidative addition. This is supported by observation of a methyl-platinum resonance in the proton spectra which has the expected ^2J(H–Pt) coupling constants for Pt(IV) species at approximately 63 Hz, indicative of both a platinum (IV) species and that the methyl group is trans to the iodide ligand, not the NHC ligand [41–44].

The Pt(IV) complexes were subsequently subjected to thermolysis in an attempt to study their reductive elimination processes. Interesting, the majority of the time, the major product formed was the original Pt(II) complex by the reductive elimination of iodomethane, the reverse of the oxidative addition mentioned above. However, in a few cases (**Pt2, Pt6** and **Pt7**), multiple unidentifiable species were observed. Cyclometalated compounds, with a methyl ligand tend to reductively elimination by C–H or C–C bond formation and less often elimination MeI. We speculate that the presence of two trans chelate ligands promote the reverse reaction of MeI elimination [45–48].

2.4. Computational studies

DFT calculations were performed to help explain the electronic transitions and photophysical spectra of all complexes. In the case of **Pt7**, these calculations were used to describe the regioselectivity of the C–H activation. The calculated LUMO orbitals are concentrated mainly on the ligand scaffold, mostly on the NHC moiety. In addition, the calculated HOMO orbitals lie predominantly on the Pt metal center, with electronic density lying on the ligands, supporting the MLCT absorption assignment [49–52](or, perhaps in some cases, mixed metal-ligand to ligand charge transfer (MM-LLCT)) [53,54]. MLCT behavior has been well documented in the literature for C~C* platinum(II) NHC complexes [55,56].

Calculations using B3LYP/LACVP** indicate that the observed isomer for **Pt7** is lower in energy than the competing isomer thus supporting the assignment of observed regioisomer of **Pt7**. This calculation involving the five-membered metallacycle incorporating the phenyl moiety places the platinum atom in a strictly planar environment. However, when this calculation was performed on the unobserved, six-membered metallacycle, the platinum atom is placed in a distorted environment. The six-membered
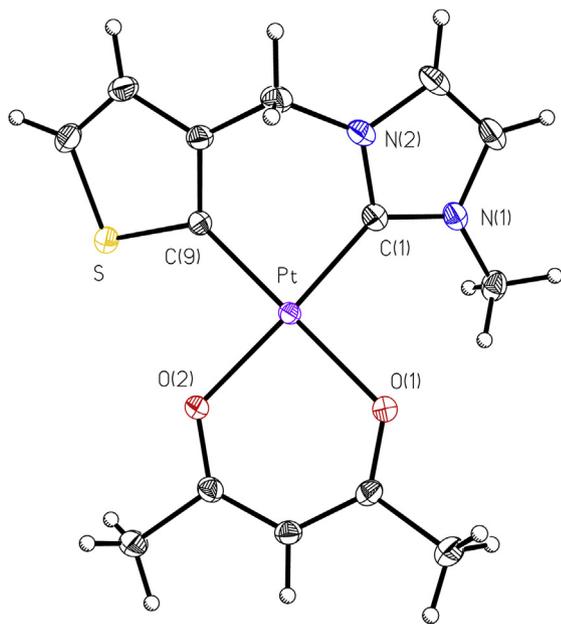
Fig. 6. ORTEP of Compound **Pt8** (50% probability thermal ellipsoids). Selected bonds lengths (Å) and angles (°): Pt–C(1): 1.964(2); Pt–C(9): 1.973(2); Pt–O(1): 2.081(1); Pt–O(2): 2.054(1); C(1)–Pt–C(9): 86.71(8); C(1)–Pt–O(2): 175.18(7); C(9)–Pt–O(2): 89.99(6); C(1)–Pt–O(1): 93.10(7); C(9)–Pt–O(1): 174.38(7); O(2)–Pt–O(1): 90.53(5).
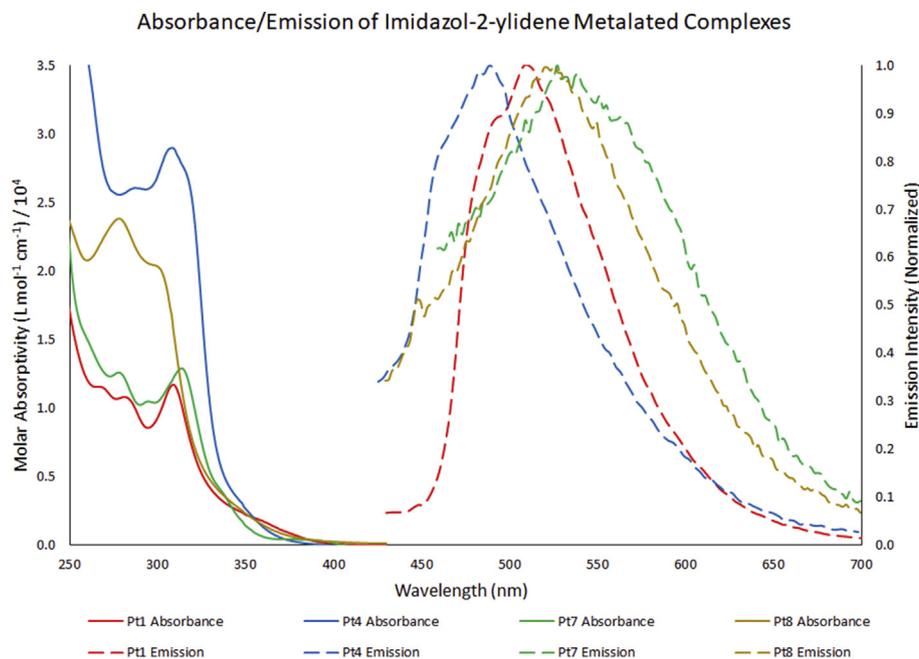
Fig. 7. Emission and absorbance spectra of **Pt1, Pt4, Pt7,** and **Pt8** complexes (Chart 1, Class A). All emission spectra used $\lambda_{ex} = 365$ nm.

metallacycle displays slight torsion of approximately 3.5°. The five-membered metallacycle planarity lowers the ground-state energy of the complex, with a computed isomer energy difference of approximately 4 kcal/mol [57].

3. Concluding remarks

Heteroleptic platinum(II) complexes bearing various NHC-based ligands were synthesized using a one-pot procedure. All complexes are blue-green emitters at room temperature and display excited-state lifetimes on the several hundred nanosecond time scale. Absorption electronic transitions were assigned as ^{3}MLCT transitions,

which were supported by DFT calculations. These complexes hold potential applications in OLED, PHOLED, and photovoltaic devices. We are currently testing these complexes as photocatalysts for a variety of processes.

4. Experimental

4.1. General considerations

3-(bromomethyl)-1-benzothiophene and 3-(bromomethyl) thiophene were purchased from Enamine Ltd. All other reagents were obtained from Sigma Aldrich. ^{1}H and ^{13}C NMR spectra were
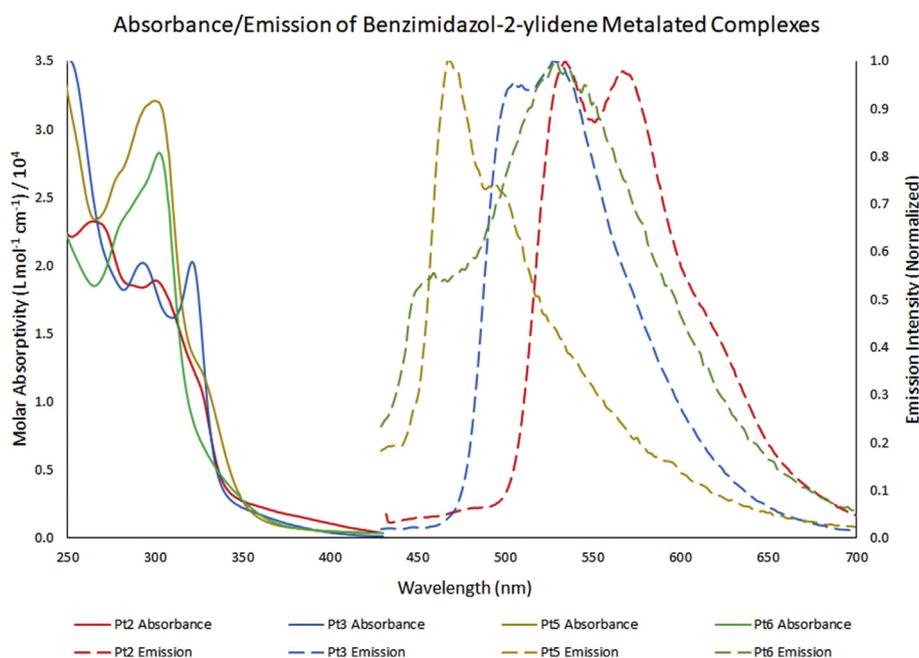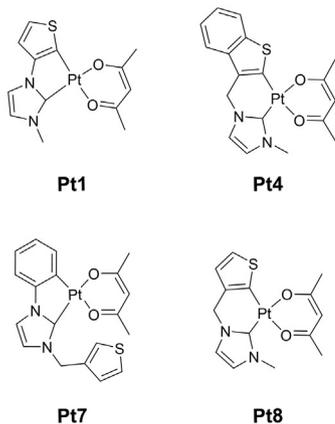

Fig. 8. Emissions and absorbances of **Pt2, Pt3, Pt5,** and **Pt6** complexes (Chart 1, Class B). All emission spectra used $\lambda_{ex} = 365$ nm.

Cyclometalated Imidazol-2-ylidenes (Class A)

Pt1   Pt4

Pt7   Pt8

Cyclometalated Benzimidazol-2-ylidenes (Class B)
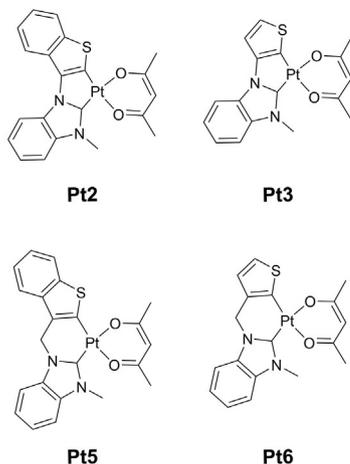
Pt2   Pt3

Pt5   Pt6

Chart 1. Metalated complexes explored in this work.

recorded at Bard College on a 400 MHz Varian spectrometer in CDCl$_3$. NMR spectra are included in the Supporting Information (S.I.)

4.2. Synthesis of ligand precursors

General Procedure: The respective boronic acid, imidazole or benzimidazole, and Cu$_2$O were introduced into a 50 mL round bottom flask with 10 mL of methanol. The solution/suspension was stirred at room temperature overnight. The suspension was filtered and the resulting solution had the majority of its solvent removed under vacuum. The remaining mixture was separated by column chromatography (CC). See S.I. for NMR spectra.

[C$_7$H$_6$N$_2$S], 1-(thiophen-3-yl)-1H-imidazole (A). 3-thienylboronic acid (0.153 g, 1.20 mmol), imidazole (0.081 g, 1.20 mmol), and Cu$_2$O (0.017 g, 0.118 mmol). CC (neat ether to 30% AcOEt/Et$_2$O). Yield: 51% (0.092 g). ^{1}H NMR: ?? = 7.14–7.16 (m, 2H, aromatic CH); 7.18–7.19 (m, 1H, aromatic CH); 7.21 (m, 1H, aromatic CH); 7.39–7.42 (m, 1H, aromatic CH); 7.79 (s, 1H, H^a).

[C$_{15}$H$_{10}$N$_2$S], 1-(benzo[b]thiophen-3-yl)-1H-benzo[d]imidazole (B). Benzo[b]thien-3-ylboronic acid (0.628 g, 3.53 mmol), benzimidazole (0.417 g, 3.53 mmol), and Cu$_2$O (0.051 g, 0.353 mmol). CC (1:1 mixture of Et$_2$O/Hexanes as an isocratic eluent). Yield: 77% (0.680 g). ^{1}H NMR: ?? = 7.31–7.43 (m, 4H, aromatic CH); 7.47–7.54 (m, 2H, aromatic CH); 7.61 (s, 1H, H^b); 7.91–7.98 (m, 2H, aromatic CH); 8.16 (s, 1H, H^a).

[C$_{11}$H$_8$N$_2$S], 1-(thiophen-3-yl)-1H-benzo[d]imidazole (C). 3-thienylboronic acid (0.302 g, 2.36 mmol), benzimidazole (0.284 g, 2.40 mmol), and Cu$_2$O (0.034 g, 0.236 mmol). CC (60%–80% Et$_2$O/Hexanes). Yield: 89% (0.420 g). ^{1}H NMR: ?? = 7.29 (dd, ^3J(H–H) = 5.1, 1.5 Hz, 1H, aromatic CH); 7.31–7.34 (m, 2H, aromatic CH); 7.39 (dd, ^3J(H–H) = 3.2, 1.5 Hz, 1H, aromatic CH); 7.50–7.54 (m, 2H, aromatic CH); 7.83–7.86 (m, 1H, aromatic CH); 8.09 (s, 1H, H^a).

4.3. Synthesis of imidazolium salts

General Procedure A: The respective ligand precursor was placed in a round bottom flask and dissolved in 10 mL of methylene
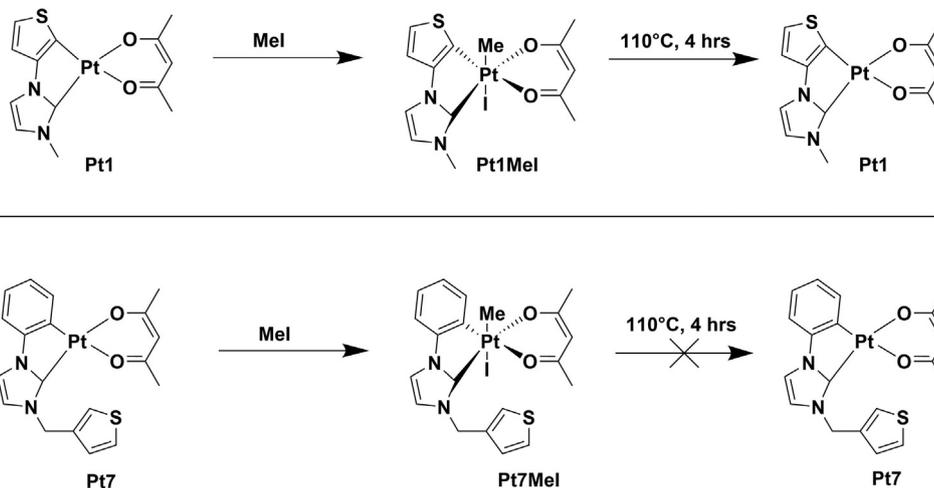
Scheme 3. Trans oxidative addition of Pt(II) complexes with iodomethane to form new Pt(IV) species. Subsequent reductive elimination of Pt(IV) complexes either formed the original Pt(II) complex or an unidentifiable mixture of isomers.

chloride. Methyl trifluoromethanesulfonate was then added to the solution. The solution was stirred under an inert atmosphere at room temperature for 90 min. The solvent was removed *in vacuo* and the product isolated as a grey-white salt.

General Procedure B: The respective bromomethyl thiophene and imidazole were mixed in 10 mL of methylene chloride to give a solution. The solution was stirred overnight at room temperature under an inert atmosphere. The solvent was removed under vacuum, resulting in a white solid.

[C$_8$H$_9$N$_2$S][CF$_3$SO$_3$], 3-methyl-1-(thiophen-3-yl)-1H-imidazole-3-ium trifluoromethanesulfonate (1). A (0.035 g, 0.233 mmol) and methyl trifluoromethanesulfonate (0.038 g, 0.233 mmol) were reacted according to general procedure A. Yield: 84% (0.061 g). ^{1}H NMR: ?? = 4.07 (s, 3H, H^g); 7.39 (dd, ^3J(H–H) = 5.3, 1.6 Hz, 1H, aromatic CH); 7.47 (t, ^3J(H–H) = 1.8 Hz, 1H, aromatic CH); 7.51 (m, 1H, aromatic CH); 7.62 (t, ^3J = 1.9 Hz, 1H, aromatic CH); 7.80 (m, 1H, aromatic CH); 9.55 (s, 1H, H^a).

[C$_{16}$H$_{13}$N$_2$S][CF$_3$O$_3$S], 1-(benzo[*b*]thiophen-3-yl)-3-methyl-1H-benzo[*d*]imidazole-3-ium trifluoromethanesulfonate (2). B (0.144 g, 0.575 mmol) and methyl trifluoromethanesulfonate (0.094 g, 0.575 mmol) were reacted according to general procedure A. Yield: 95% (0.224 g). ^{1}H NMR: ?? = 4.34 (s, 3H, H^k) 7.44–7.48 (m, 3H, aromatic CH); 7.50–7.54 (m, 1H, aromatic CH); 7.63 (t, ^3J(H–H) = 8.0 Hz, 1H, aromatic CH); 7.74 (t, ^3J(H–H) = 7.8 Hz, 1H, aromatic CH); 7.86 (d, ^3J(H–H) = 8.4 Hz, 1H, aromatic CH); 7.99 (d, ^3J(H–H) = 8.2 Hz, 1H, aromatic CH); 8.26 (s, 2H, H^b); 9.86 (s, 1H, H^a).

[C$_{12}$H$_{11}$N$_2$S][CF$_3$SO$_3$], 3-methyl-1-(thiophen-3-yl)-1H-benzo[*d*]imidazole-3-ium trifluoromethanesulfonate (3). C (0.130 g, 0.649 mmol) and methyl trifluoromethanesulfonate (0.097 g, 0.649 mmol) were reacted according to general procedure A. Yield: 95% (0.224 g). ^{1}H NMR: ?? = 4.30 (s, 3H, H^i); 7.48 (d, ^3J(H–H) = 5.2 Hz, 1H, aromatic CH); 7.62–7.82 (m, 5H, aromatic CH); 7.97 (s, 1H, H^b); 9.98 (s, 1H, H^a).

[C$_{13}$H$_{13}$N$_2$S][Br], 1-(benzo[*b*]thiophen-3-ylmethyl)-3-methyl-1H-imidazole-3-ium bromide (4): 3-(bromomethyl)-1-benzothiophene (0.150 g, 0.660 mmol) and 1-methylimidazole (0.054 g, 0.660 mmol) were reacted according to general procedure B. Yield: 94% (0.230 g). ^{1}H NMR: ?? = 6.14 (s, 2H, H^b); 7.26–7.40 (m, 5H, aromatic CH); 7.65 (dd, ^3J(H–H) = 8.3, 1.5 Hz, 1H, aromatic CH); 7.71 (t, ^3J(H–H) = 1.9 Hz, 1H, aromatic CH); 7.78 (dd, ^3J(H–H) = 7.1, 1.3 Hz, 1H, aromatic CH); 7.87 (t, ^3J(H–H) = 1.9 Hz, 1H, aromatic CH); 8.16 (dd, ^3J(H–H) = 7.3, 1.6 Hz, 1H, aromatic CH); 8.27 (s, 1H, H^c); 10.97 (s, 1H, H^a).

[C$_{17}$H$_{15}$N$_2$S][Br], 1-(benzo[*b*]thiophen-3-ylmethyl)-3-methyl-1H-benzo[*d*]imidazole-3-ium bromide (5). 3-(bromomethyl)-1-benzothiophene (0.286 g, 1.26 mmol) and 1-methylbenzimidazole (0.167 g, 1.26 mmol) were reacted according to general procedure B. Yield: 84% (0.381 g). ^{1}H NMR: ?? = 4.21 (s, 3H, H^l); 6.08 (s, 2H, H^b) 7.41 (m, 2H, aromatic CH); 7.65 (m, 4H, aromatic CH); 7.86 (d, ^3J(H–H) = 8.0 Hz, 1H, aromatic CH); 7.91 (s, 1H, H^c); 7.95 (d, ^3J(H–H) = 7.9 Hz, 1H, CH); 11.59 (s, 1H, H^a).

[C$_{13}$H$_{13}$N$_2$S][Br], 3-methyl-1-(thiophen-3-ylmethyl)-1H-benzo[*d*]imidazole-3-ium bromide (6). 3-(bromomethyl)thiophene (0.150 g, 0.847 mmol) and 1-methylbenzimidazole (0.112 g, 0.847 mmol) were reacted according to general procedure B. Yield: 97% (0.264 g). ^{1}H NMR: ?? = 4.25 (s, 3H, H^j); 5.88 (s, 2H, H^b) 7.30 (m, 1H, aromatic CH); 7.57–7.69 (m, 5H, H^c, aromatic CH); 11.60 (s, 1H, H^a).

[C$_{14}$H$_{13}$N$_2$S][Br], 3-phenyl-1-(thiophen-3-ylmethyl)-1H-imidazole-3-ium bromide (7). 3-(bromomethyl)thiophene (0.150 g, 0.847 mmol) and 1-phenylbenzimidazole (0.122 g, 0.847 mmol) were reacted according to general procedure B. Yield: 100% (0.271 g). ^{1}H NMR: ?? = 5.82 (s, 2H, H^b); 7.23–7.26 (m, 1H, H^e); 7.35 (dd, ^3J(H–H) = 5.0, 1.3 Hz, 1H, H^d); 7.38–7.48 (m, 4H, aromatic CH); 7.65–7.72 (m, 3H, H^g, aromatic CH); 7.82–7.86 (m, 2H, H^f,

aromatic CH); 10.91 (s, 1H, H^a).

[C$_8$H$_8$NS$_2$][Br], 3-methyl-1-(thiophen-3-ylmethyl)-1H-imidazole-3-ium bromide (8): 3-(bromomethyl)thiophene (0.155 g, 0.877 mmol) and 1-methylimidazole (0.072 g, 0.877 mmol) were reacted according to general procedure B. Yield: 85% (0.193 g). ^{1}H NMR: ?? = 4.03 (s, 3H, H^h); 5.61 (s, 2H, H^b); 7.19 (d, ^3J(H–H) = 5.0 Hz, 1H, aromatic CH); 7.31–7.38 (m, 3H, aromatic CH); 7.66 (d, ^3J(H–H) = 3.0 Hz, 1H, aromatic CH); 10.48 (s, 1H, H^a).

4.4. Synthesis of cyclometalated complexes

General Procedure: The respective imidazolium salt, 10 equivalents of K$_2$CO$_3$, and one equivalent of *cis*-dichlorobis(dimethyl sulfoxide)platinum(II) or dichloro(1,5-cyclooctadiene)platinum(II) were dissolved/suspended in 10 mL of methylene chloride. The mixture was stirred overnight at room temperature under an inert atmosphere. The solvent was removed *in vacuo*. Subsequently, acetylacetone and 10 mL of DMF were added to the flask. The mixture was heated to 110 °C for 4 h under an inert atmosphere. The solvent was then removed *in vacuo*. 20 mL of methylene chloride was added to the flask and the solution filtered to remove the particulate matter. The desired complex was isolated by column chromatography.

[C$_{13}$H$_{15}$N$_2$O$_2$PtS], Pt1: Ligand **1** (0.097 g, 0.308 mmol), K$_2$CO$_3$ (0.426 g, 3.08 mmol), dichloro(1,5-cyclooctadiene)platinum(II) (0.115 g, 0.308 mmol), and acetylacetone (0.124 g, 1.24 mmol). CC (100% methylene chloride). Yield: 21% (0.030 g). ^{1}H NMR: ?? = 1.95 (s, 3H, CH$_3$); 2.01 (s, 3H, CH$_3$); 4.04 (s, 3H, H^e); 5.50 (s, 1H, H^g); 6.72 (d, ^4J(Pt–H) = 13.6 Hz, ^3J(H–H) = 5.0 Hz, 1H, H^d); 6.96 (d, ^3J(H–H) = 4.8 Hz, 1H, aromatic CH); 7.10–7.12 (m, ^4J(Pt–H) = 31.3 Hz, 2H, H^c, aromatic CH). ^{13}C NMR (101 MHz): δ = 184.79, 183.89, 145.77, 144.65, 122.96, 119.86, 118.70, 115.01, 113.32, 101.99, 34.82, 27.74, 27.49. Calculated: *m/z* [458.0502], Found: *m/z* [458.0520].

[C$_{21}$H$_{19}$N$_2$O$_2$PtS], Pt2: Ligand **2** (0.061 g, 0.145 mmol), K$_2$CO$_3$ (0.200 g, 1.45 mmol), dichloro(1,5-cyclooctadiene)platinum(II) (0.054 g, 0.145 mmol), and acetylacetone (0.058 g, 0.580 mmol). CC (100% methylene chloride). Yield: 31% (0.033 g). ^{1}H NMR: ?? = 2.06 (s, 3H, CH$_3$); 2.10 (s, 3H, CH$_3$); 4.33 (s, 3H, H^a); 5.59 (s, 1H, H^k); 7.16 (t, ^3J(H–H) = 7.5 Hz, 1H, aromatic CH); 7.32–7.44 (m, 4H, aromatic CH); 7.83 (d, ^3J(H–H) = 7.9 Hz, 1H, aromatic CH); 8.25 (t, ^3J(H–H) = 8.9 Hz, 2H, aromatic CH). ^{13}C NMR (101 MHz): δ = 185.18, 184.62, 158.32, 141.58, 138.21, 134.64, 131.10, 130.25, 128.14, 124.00, 123.69, 123.59, 122.18, 120.49, 118.85, 112.74, 110.50, 102.20, 31.44, 27.82, 27.43. ESI-MS (*m/z*): Calculated: *m/z* [558.0815], Found: *m/z* [558.0845].

[C$_{17}$H$_{17}$N$_2$O$_2$PtS], Pt3: Ligand **3** (0.224 g, 0.615 mmol), K$_2$CO$_3$ (0.850 g, 6.15 mmol), dichloro(1,5-cyclooctadiene)platinum(II) (0.230 g, 0.615 mmol), and acetylacetone (0.246 g, 2.46 mmol). CC (100% methylene chloride). Yield: 28% (0.087 g). ^{1}H NMR: ?? = 2.03 (s, 3H, CH$_3$); 2.06 (s, 3H, CH$_3$); 4.28 (s, 3H, H^a); 5.55 (s, 1H, H^i); 7.24–7.39 (m, 5H, H^b, aromatic CH); 7.69 (d, ^3J(H–H) = 7.9 Hz, 1H, aromatic CH). ^{13}C NMR (101 MHz): δ = 184.92, 184.29, 156.59, 144.03, 134.54, 130.27, 124.17, 123.02, 122.19, 118.88, 114.00, 110.45, 110.29, 102.06, 31.28, 27.80, 27.41.

[C$_{18}$H$_{19}$N$_2$O$_2$PtS], Pt4: Ligand **4** (0.200 g, 0.645 mmol), K$_2$CO$_3$ (0.894 g, 6.45 mmol), *cis*-dichlorobis(dimethyl sulfoxide)platinum(II) (0.273 g, 0.645 mmol), and acetylacetone (0.259 g, 2.59 mmol). CC (100% methylene chloride). Yield: 21% (0.072 g). Suitable crystals for X-ray diffraction grown by slow evaporation of methylene chloride. ^{1}H NMR: ?? = 1.94 (s, 3H, CH$_3$); 2.04 (s, 3H, CH$_3$); 3.95 (s, 3H, H^a); 5.20 (s, 2H, H^d); 5.51 (s, ^4J(Pt–H) = 26.6 Hz, 1H, H^j); 6.81 (d, ^3J(H–H) = 5.6 Hz, 1H, H^b); 7.01 (d, ^3J(H–H) = 4.9 Hz, 1H, H^c); 7.06 (t, ^3J(H–H) = 7.7 Hz, 1H, H^g); 7.20 (t, ^3J(H–H) = 7.6 Hz, 1H, H^f); 7.43 (d, ^3J(H–H) = 8.0 Hz, 1H, H^e); 7.77 (d, ^3J(H–H) = 7.9 Hz,

1H, H^h). ^{13}C NMR (101 MHz): δ = 185.59, 184.35, 143.00, 141.27, 138.64, 126.36, 124.34, 122.86, 122.71, 122.09, 121.50, 120.84, 120.78, 117.75, 102.06, 50.09, 36.92, 27.54. Calculated: m/z [522.0815], Found: m/z [522.0819].

[C$_{22}$H$_{21}$N$_2$O$_2$PtS], Pt5: Ligand **5** (0.381 g, 1.06 mmol), K$_2$CO$_3$ (1.47 g, 10.6 mmol), cis-dichlorobis(dimethyl sulfoxide)platinum(II) (0.448 g, 1.06 mmol), and acetylacetone (0.425 g, 4.25 mmol). CC (100% methylene chloride) Yield: 21% (0.133 g). ^{1}H NMR: ?? = 1.99 (s, 3H, CH$_3$); 2.08 (s, 3H, CH$_3$); 4.14 (s, 3H, H^a); 5.42 (s, 2H, H^f); 5.56 (s, 1H, H^l); 7.09 (t, ^3J(H–H) = 7.4 Hz, 1H, H^i); 7.21–7.39 (m, 4H, H^{b,c,e,h}); 7.55 (m, 2H, H^{d,g}); 7.80 (d, ^3J(H–H) = 7.9 Hz, 1H, H^i). ^{13}C NMR (101 MHz): δ = 185.80, 184.74, 152.99, 143.08, 138.65, 134.85, 133.72, 126.41, 126.06, 123.41, 123.20, 122.81, 122.15, 120.98, 117.90, 110.23, 109.91, 102.15, 45.96, 33.71, 27.60, 27.47. Calculated: m/z [572.0971], Found: m/z [572.0972].

[C$_{18}$H$_{19}$N$_2$O$_2$PtS], Pt6: Ligand **6** (0.264 g, 0.854 mmol), K$_2$CO$_3$ (1.18 g, 8.54 mmol), cis-dichlorobis(dimethyl sulfoxide)platinum(II) (0.360 g, 0.854 mmol), and acetylacetone (0.342 g, 3.42 mmol). CC (100% methylene chloride). Yield: 32% (0.143 g). ^{1}H NMR: ?? = 1.96 (s, 3H, CH$_3$); 2.04 (s, 3H, CH$_3$); 4.11 (s, 3H, H^a); 5.25 (s, 2H, H^f); 5.52 (s, 1H, H^j); 7.00 (d, ^4J(Pt–H) = 14.8 Hz, ^3J(H–H) = 5.0 Hz, 1H, H^g); 7.23–7.36 (m, 4H, aromatic CH); 7.43 (d, ^3J(H–H) = 14.8 Hz, 1H, H^e). ^{13}C NMR (101 MHz): δ = 185.66, 184.58, 152.76, 134.81, 133.70, 132.72, 125.35, 125.27, 123.26, 123.04, 120.55, 110.11, 109.82, 102.01, 47.82, 33.60, 27.62, 27.49. Calculated: m/z [522.0815], Found: m/z [522.0844].

[C$_{19}$H$_{19}$N$_2$O$_2$PtS], Pt7: Ligand **7** (0.203 g, 0.632 mmol), K$_2$CO$_3$ (0.876 g, 6.32 mmol), dichloro(1,5-cyclooctadiene)platinum(II) (0.236 g, 0.632 mmol), and acetylacetone (0.253 g, 2.53 mmol). CC (100% methylene chloride). Yield: 23% (0.078 g). Suitable crystals for X-ray diffraction grown by vial-in-a-vial vapor diffusion using methylene chloride and pentane. ^{1}H NMR: ?? = 1.86 (s, 3H, CH$_3$); 2.04 (s, 3H, CH$_3$); 5.48 (s, 1H, H^l); 5.70 (s, 2H, H^h); 6.78 (d, ^4J(Pt–H) = 12.3 Hz, ^3J(H–H) = 2.1 Hz, 1H, H^i); 6.89–6.92 (m, 1H, aromatic CH); 6.97–7.02 (m, 2H, CH, H^f); 7.17–7.21 (m, 2H, CH, H^j); 7.26–7.28 (m, 1H, aromatic CH); 7.31 (s, 1H, H^a); 7.78 (d, ^3J(Pt–H) = 54.2 Hz, ^3J(H–H) = 6.7 Hz, 1H, H^e). ^{13}C NMR (101 MHz): δ = 185.18, 184.75, 149.60, 146.76, 137.79, 131.55, 127.47, 126.56, 124.73, 124.15, 123.48, 119.27, 114.67, 109.99, 102.02, 46.13, 27.87, 23.72. Calculated: m/z [534.0815], Found: m/z [534.0836].

[C$_{14}$H$_{17}$N$_2$O$_2$PtS], Pt8: Ligand **8** (0.193 g, 0.745 mmol), K$_2$CO$_3$ (1.03 g, 7.45 mmol), dichloro(1,5-cyclooctadiene)platinum(II) (0.278 g, 0.745 mmol), and acetylacetone (0.298 g, 2.98 mmol). CC (100% methylene chloride). Yield: 54% (0.191 g). Suitable crystals for X-ray diffraction grown by layer-by-layer diffusion of CDCl$_3$ and pentane. ^{1}H NMR: ?? = 1.91 (s, 3H, CH$_3$); 1.99 (s, 3H, CH$_3$); 3.92 (s, 3H, H^a); 5.02 (s, 2H, H^d); 5.48 (s, 1H, H^h); 6.78 (s, 1H, H^b); 6.90–6.93 (m, 2H, H^{c,e}); 7.20 (d, ^4J(Pt–H) = 26.1 Hz, ^3J(H–H) = 4.9 Hz, 1H, H^f). ^{13}C NMR (101 MHz): δ = 185.45, 184.18, 140.91, 133.02, 125.18, 124.97, 121.24, 120.69, 120.47, 101.95, 52.04, 36.82, 27.57, 27.52. Calculated: m/z [472.0658], Found: m/z [472.0666].

4.5. Photophysical properties of cyclometalated Pt(II) complexes

Emission spectra and lifetime measurements were recorded at Bard College on a PTI QuantaMaster 400 device and analyzed using PTI FelixGX software. Absorbance spectra were recorded on an Agilent Technologies Cary Series UV-Vis spectrophotometer at Bard College. All absorbance and emission photophysical studies were run at 0.10 mM concentrations in methylene chloride. Lifetime samples were also prepared in methylene chloride and degassed for 5 min with argon.

4.6. Oxidative addition and reductive elimination studies

General Procedure for Oxidative Addition: One equivalent of the respective cyclometalated Pt(II) complex and 100 equivalents of iodomethane were dissolved in 10 mL of acetone. The mixture was refluxed for 2 h under an inert atmosphere. The solvent was then removed in vacuo and the complex isolated as yellow-white solid.

General Procedure for Reductive Elimination: The respective Pt(IV) metalated complex was dissolved in 10 mL of toluene. The mixture was refluxed for 4 h under an inert atmosphere. The solvent was the removed in vacuo and the complex isolated as a yellow-brown solid. Extent of reaction estimated using peak integration in the ^{1}H NMR spectra.

Pt1MeI: Pt1 (0.007 g, 15.27 μmol) and iodomethane (0.217 g, 1.53 mmol). ^{1}H NMR: ?? = 1.24 (s, 3H, ^2J(Pt–H) = 62.7 Hz); 2.06 (s, 3H); 2.12 (s, 3H); 4.12 (s, 3H); 5.52 (s, 1H); 6.93–8.00 (aromatics, 4H). **Pt1MeI** formed in 100% conversion upon oxidative addition with iodomethane. Original Pt(II) complex was formed upon refluxing with toluene in 85% conversion. Compound was characterized using ^{1}H NMR of **Pt1**.

Pt2MeI: Pt2 (0.007 g, 15.27 μmol) and iodomethane (0.217 g, 1.53 mmol). ^{1}H NMR: ?? = 1.27 (s, 3H, ^2J(Pt–H) = 63.1 Hz); 2.14 (s, 3H); 2.19 (s, 3H); 4.40 (s, 3H, ^4J(Pt–H) = 4.1 Hz); 5.58 (s, 1H, ^4J(Pt–H) = 4.2 Hz); 7.39–8.42 (aromatics, 8H). **Pt2MeI** formed in 93% conversion upon oxidative addition with iodomethane. Original Pt(II) complex did not form upon refluxing with toluene.

Pt3MeI: Pt3 (0.005 g, 9.83 μmol) and iodomethane (0.140 g, 0.98 mmol). ^{1}H NMR: ?? = 1.29 (s, 3H, ^2J(Pt–H) = 63.1 Hz); 2.12 (s, 3H); 2.16 (s, 3H); 4.36 (s, 3H, ^4J(Pt–H) = 4.1 Hz); 5.57 (s, 1H, ^4J(Pt–H) = 4.3 Hz); 7.38–7.84 (aromatics, 6H). **Pt3MeI** formed in 87% conversion upon oxidative addition with iodomethane. Original Pt(II) complex did not form upon refluxing with toluene.

Pt4MeI: Pt4 (0.007 g, 15.27 μmol) and iodomethane (0.217 g, 1.53 mmol). ^{1}H NMR: ?? = 1.60 (s, 3H, ^2J(Pt–H) = 63.3 Hz); 2.06 (s, 3H); 2.16 (s, 3H); 4.14 (s, 3H, ^4J(Pt–H) = 4.0 Hz); 5.34, 5.66 (ABq, 2H, J_{AB}(H–H) = 15.2 Hz, ^4J(Pt–H) = 14.5 Hz); 5.56 (s, 1H, ^4J(Pt–H) = 3.7 Hz); 6.90–7.80 (aromatics, 6H). **Pt4MeI** formed in 96% conversion upon oxidative addition with iodomethane. Original Pt(II) complex was formed upon refluxing with toluene in 85% conversion. Compound was characterized using ^{1}H NMR of **Pt4**.

Pt5MeI: Pt5 (0.015 g, 26.11 μmol) and iodomethane (0.371 g, 2.61 mmol). ^{1}H NMR: ?? = 1.68 (s, 3H, ^2J(Pt–H) = 63.4 Hz); 2.11 (s, 3H); 2.20 (s, 3H); 4.36 (s, 3H); 5.60, 5.86 (ABq, 2H, J_{AB}(H–H) = 15.2 Hz, ^4J(Pt–H) = 14.7 Hz); 5.60 (s, 1H); 7.13–7.81 (aromatics, 8H). **Pt5MeI** formed in 82% conversion upon oxidative addition with iodomethane. Original Pt(II) complex was formed upon refluxing with toluene in 95% conversion. Compound was characterized using ^{1}H NMR of **Pt5**.

Pt6MeI: Pt6 (0.005 g, 9.57 μmol) and iodomethane (0.136 g, 0.96 mmol). ^{1}H NMR: ?? = 1.67 (s, 3H, ^2J(Pt–H) = 62.9 Hz); 2.09 (s, 3H); 2.16 (s, 3H); 4.32 (s, 3H, ^4J(Pt–H) = 3.8 Hz); 5.40, 5.71 (ABq, 2H, J_{AB}(H–H) = 15.3 Hz, ^4J(Pt–H) = 14.8 Hz); 5.57 (s, 1H, ^4J(Pt–H) = 3.8 Hz); 6.90–7.58 (aromatics, 6H). **Pt6MeI** formed in 86% conversion upon oxidative addition with iodomethane. Original Pt(II) complex was formed upon refluxing with toluene in 49% conversion. Compound was characterized using ^{1}H NMR of **Pt6**.

Pt7MeI: Pt7 (0.008 g, 14.97 μmol) and iodomethane (0.212 g, 1.50 mmol). ^{1}H NMR: ?? = 1.13 (s, 3H, ^2J(Pt–H) = 63.2 Hz); 2.01 (s, 3H); 2.16 (s, 3H); 5.51 (s, 1H, ^4J(Pt–H) = 4.2 Hz); 5.67, 5.97 (ABq, 2H, J_{AB}(H–H) = 14.5 Hz); 6.96–7.80 (aromatics, 9H). **Pt7MeI** formed in 100% conversion upon oxidative addition with iodomethane. Original Pt(II) complex did not form upon refluxing with toluene.

Pt8MeI: Pt8 (0.010 g, 21.17 μmol) and iodomethane (0.300 g,

2.12 mmol). ^{1}H NMR: ?? = 1.58 (s, 3H, ^2J(Pt−H) = 63.8 Hz); 2.05 (s, 3H); 2.12 (s, 3H); 4.11 (s, 3H); 5.09, 5.54 (ABq, 2H, J_{AB}(-H−H) = 14.8 Hz, ^4J(Pt−H) = 9.0 Hz); 5.52 (s, 1H); 6.81−7.28 (aromatics, 4H). **Pt8MeI** formed in 96% conversion upon oxidative addition with iodomethane. Original Pt(II) complex was formed upon refluxing with toluene in 85% conversion. Compound was characterized using ^{1}H NMR of **Pt8**.

4.7. X-ray diffraction (XRD)

X-ray diffraction data were collected on a Bruker APEX 2 CCD platform diffractometer (Mo K??(λ = 0.71073 Å)) at 125 K. The structure was solved using direct methods and standard difference map techniques, and was refined by full-matrix least-squares procedures on F2 with SHELXTL2014 [58]. See Supplementary Information and Figs. 2−6 for ORTEP drawing, labels, bond lengths, and bond angles. Crystallographic data have been deposited with the Cambridge Crystallographic Data Centre, CCDC numbers 1875652, 1875653, 1875654, 1875655, and 1875656.

4.8. Mass spectrometry

All compounds were dissolved in $CHCl_3$ and were analyzed using an Agilent 6520 electrospray ionization quadrupole time-of-flight mass spectrometer. Using an Agilent 1100 HPLC system, 10 μL of sample was injected using $CHCl_3$ as the mobile phase and a flow rate of 0.4 mL/min. Samples were ionized by electrospray ionization in the positive mode.

4.9. Computational details

Calculations were performed using the *Jaguar* version 10.0 suite of ab initio software packages. The density functional hybrid B3LYP was used with the LACVP** basis set. The LACVP** basis set includes an effective core potential (ECP). Each reported structure was optimized to ground-state minimum as confirmed by absence of negative eigenvalues in the vibrational frequency analysis.

Acknowledgments

Appendix A. Supplementary data

Supplementary data to this article can be found online at https://doi.org/10.1016/j.jorganchem.2018.10.026.

References

[1] D.J.D. Wilson, S.A. Couchman, J.L. Dutton, Are N-heterocyclic carbenes "better" ligands than phosphines in main group chemistry? A theoretical case study of ligand-stabilized E $_2$ molecules, L-E-E-L (L = NHC, phosphine; E = C, Si, Ge, Sn, Pb, N, P, as, Sb, Bi), Inorg. Chem. 51 (2012) 7657−7668, https://doi.org/10.1021/ic300686n.

[2] W.A. Herrmann, N-heterocyclic carbenes: a new concept in organometallic catalysis, Angew. Chem. Int. Ed. 41 (2002) 1290−1309, https://doi.org/10.1002/1521-3773(20020415)41:8<1290::AID-ANIE1290>3.0.CO;2-Y.

[3] N. Fröhlich, U. Pidun, M. Stahl, G. Frenking, Carbenes as Pure Donor Ligands: Theoretical Study of Beryllium−Carbene Complexes 1, 1997, https://doi.org/10.1021/OM960752V.

[4] F.E. Hahn, M.C. Jahnke, Heterocyclic carbenes: synthesis and coordination chemistry, Angew. Chem. Int. Ed. 47 (2008) 3122−3172, https://doi.org/10.1002/anie.200703883.

[5] E. Chardon, G. Dahm, G. Guichard, S. Bellemin-Laponnaz, Exploring nitrogen ligand diversity in trans-N-heterocyclic carbene-amine platinum complexes: synthesis, characterization, and application to fluorescence, Chem. Asian J. 8 (2013) 1232−1242, https://doi.org/10.1002/asia.201201148.

[6] G.F. Silbestri, J.C. Flores, E. de Jesús, Water-soluble N-heterocyclic carbene platinum(0) complexes: recyclable catalysts for the hydrosilylation of alkynes in water at room temperature, Organometallics 31 (2012) 3355−3360, https://doi.org/10.1021/om300148q.

[7] A.A. Makarova, E.V. Grachova, D. Niedzialek, A.I. Solomatina, S. Sonntag, A.V. Fedorov, O.Y. Vilkov, V.S. Neudachina, C. Laubschat, S.P. Tunik, D.V. Vyalikh, A curious interplay in the films of N-heterocyclic carbene Pt(II) complexes upon deposition of alkali metals, Sci. Rep. 6 (2016) 25548, https://doi.org/10.1038/srep25548.

[8] T. Fleetham, G. Li, J. Li, Phosphorescent Pt(II) and Pd(II) complexes for efficient, high-color-quality, and stable OLEDs, Adv. Mater. 29 (2017) 1−16, https://doi.org/10.1002/adma.201601861.

[9] R. Visbal, M.C. Gimeno, N-heterocyclic carbene metal complexes: photoluminescence and applications, Chem. Soc. Rev. 43 (2014) 3551−3574, https://doi.org/10.1039/C3CS60466G.

[10] W.C.H. Choy, W.K. Chan, Y. Yuan, Recent advances in transition metal complexes and light-management engineering in organic optoelectronic devices, Adv. Mater. 26 (2014) 5368−5399, https://doi.org/10.1002/adma.201306133.

[11] H. Yersin, A.F. Rausch, R. Czerwieniec, T. Hofbeck, T. Fischer, The triplet state of organo-transition metal compounds. Triplet harvesting and singlet harvesting for efficient OLEDs, Coord. Chem. Rev. 255 (2011) 2622−2652, https://doi.org/10.1016/J.CCR.2011.01.042.

[12] F. Aznarez, P.J. Sanz Miguel, T.T.Y. Tan, F.E. Hahn, Preparation of rhodium(III) di-NHC chelate complexes featuring two different NHC donors via a mild NaOAc-assisted C−H activation, Organometallics 35 (2016) 410−419, https://doi.org/10.1021/acs.organomet.5b00993.

[13] S.K. Yen, L.L. Koh, F. Ekkehardt Hahn, H.V. Huynh, T.S. Andy Hor, Convenient Entry to Mono- or Dinuclear Palladium(II) Benzothiazolin-2-ylidene Complexes and Their Activities toward Heck Coupling, 2006, https://doi.org/10.1021/OM060510N.

[14] H.V. Huynh, N. Meier, T. Pape, F.E. Hahn, Benzothiazolin-2-ylidene Complexes of Iridium(I), 2006, https://doi.org/10.1021/OM060006I.

[15] Y. Unger, D. Meyer, O. Molt, C. Schildknecht, I. Münster, G. Wagenblast, T. Strassner, Green-blue emitters: NHC-based cyclometalated [Pt(C^C*)(acac)] complexes, Angew. Chem. Int. Ed. 49 (2010) 10214−10216, https://doi.org/10.1002/anie.201001316.

[16] Y. Luo, Z. Chen, J. Zhang, Y. Tang, Z. Xu, D. Tang, A cyclometalated (C^C*) platinum(ii) NHC complex decorated via different carboranes to tune the photodeactivation mechanism: a theoretical investigation, RSC Adv. 6 (2016) 113513−113521, https://doi.org/10.1039/C6RA18631A.

[17] H. Leopold, I. Císařová, T. Strassner, Phosphorescent C^C cyclometalated thiazol-2-ylidene iridium(III) complexes: synthesis, structure, and photophysics, Organometallics 36 (2017) 3016−3018, https://doi.org/10.1021/acs.organomet.7b00421.

[18] A. Tronnier, A. Pöthig, S. Metz, G. Wagenblast, I. Münster, T. Strassner, Enlarging the π system of phosphorescent (C^C*) cyclometalated platinum(II) NHC complexes, Inorg. Chem. 53 (2014) 6346−6356, https://doi.org/10.1021/ic500971z.

[19] I.S. Lee, D.S. Choi, D.M. Shin, Y.K. Chung, C.H. Choi, Preparation of Thiophene-coordinated Ruthenium Complexes for Nonlinear Optics, 2004, https://doi.org/10.1021/OM034324I.

[20] Y. Cao, Y. Bai, Q. Yu, Y. Cheng, S. Liu, D. Shi, F. Gao, P. Wang, Dye-sensitized solar cells with a high absorptivity ruthenium sensitizer featuring a 2-(hexylthio)thiophene conjugated bipyridine, J. Phys. Chem. C 113 (2009) 6290−6297, https://doi.org/10.1021/jp9006872.

[21] T. Kollek, D. Wurmbrand, S.T. Birkhold, E. Zimmermann, J. Kalb, L. Schmidt-Mende, S. Polarz, Thiophene-functionalized hybrid perovskite microrods and their application in photodetector devices for investigating charge transport through interfaces in particle-based materials, ACS Appl. Mater. Interfaces 9 (2017) 1077−1085, https://doi.org/10.1021/acsami.6b12466.

[22] C. Anderson, M. Crespo, F.D. Rochon, Stereoselective oxidative addition of methyl iodide to chiral cyclometallated platinum(II) compounds derived from (R)-(+)-1-(1-naphthylethylamine). Crystal structure of [PtMe{3-(R)-(C$_{10}$H$_7$) CHMeNCHC$_4$H$_2$S)PPh$_3$], J. Organomet. Chem. 631 (2001) 164−174, https://doi.org/10.1016/S0022-328X(01)01043-9.

[23] C. Anderson, M. Crespo, J. Morris, J.M. Tanski, Reactivity of cyclometallated platinum complexes with chiral ligands, J. Organomet. Chem. 691 (2006) 5635−5641, https://doi.org/10.1016/J.JORGANCHEM.2006.09.012.

[24] C. Anderson, M. Crespo, M. Font-Bardıa, X. Solans, Oxidative addition of alkyl halides to chiral cyclometallated platinum(II) complexes with thienyl imines. X-ray crystal structure of [PtMe{3-((S)-PhCHMeNCH)C$_4$H$_2$S}SMe$_2$], J. Organomet. Chem. 604 (2000) 178−185, https://doi.org/10.1016/S0022-328X(00)00231-X.

[25] T. Kesharwani, K.A. Giraudy, J.L. Morgan, C. Kornman, A.D. Olaitan, Green synthesis of halogenated thiophenes, selenophenes and benzo[b]selenophenes using sodium halides as a source of electrophilic halogens, Tetrahedron Lett. 58 (2017) 638−641, https://doi.org/10.1016/j.tetlet.2017.01.007.

[26] T. Kesharwani, C.T. Kornman, A.L. Tonnaer, A.D. Royappa, Green synthesis of benzo[b]thiophenes via iron(III) mediated 5-endo-dig iodocyclization of 2-alkynylthioanisoles, Tetrahedron Lett. 57 (2016) 411−414, https://doi.org/10.1016/j.tetlet.2015.12.037.

[27] C.M. Anderson, N. Oh, T.A. Balema, F. Mastrocinque, C. Mastrocinque, D. Santos, M.W. Greenberg, J.M. Tanski, Regioselective C–H/C–X activation of naphthyl-derived ligands to form six-membered palladacycles, Tetrahedron Lett. 57 (2016) 4574–4577, https://doi.org/10.1016/j.tetlet.2016.08.092.

[28] C.M. Anderson, M.W. Greenberg, T.A. Balema, L.M. Duman, N. Oh, A. Hashmi, L. Ladner, K. Jain, D. Yu, J.M. Tanski, Regioselective formation of six-membered platinacycles by C–X and C–H oxidative addition, Tetrahedron Lett. 56 (2015) 6352–6355, https://doi.org/10.1016/J.TETLET.2015.09.121.

[29] I. Omae, Applications of cyclometalation reaction five-membered ring products, J. Organomet. Chem. 869 (2018) 88–105, https://doi.org/10.1016/J.JORGANCHEM.2018.05.015.

[30] I. Omae, Applications of six-membered ring products from cyclometalation reactions, J. Organomet. Chem. 848 (2017) 184–195, https://doi.org/10.1016/J.JORGANCHEM.2017.07.035.

[31] C.M. Anderson, M.W. Greenberg, L. Spano, L. Servatius, J.M. Tanski, Regioselective competition between the formation of seven-membered and five-membered cyclometalated platinacycles preceded by Csp^2Csp^3 reductive elimination, J. Organomet. Chem. 819 (2016) 27–36, https://doi.org/10.1016/J.JORGANCHEM.2016.06.018.

[32] C.M. Anderson, M. Crespo, N. Kfoury, M.A. Weinstein, J.M. Tanski, Regioselective C–H activation preceded by $C_{sp}^2-C_{sp}^3$ reductive elimination from cyclometalated platinum(IV) complexes, Organometallics 32 (2013) 4199–4207, https://doi.org/10.1021/om400398g.

[33] M. Crespo, C.M. Anderson, N. Kfoury, M. Font-Bardia, T. Calvet, Reductive elimination from cyclometalated platinum(IV) complexes to form $c_{sp}^2-c_{sp}^3$ bonds and subsequent competition between C_{sp}^2–H and C_{sp}^3–H bond activation, Organometallics 31 (2012) 4401–4404, https://doi.org/10.1021/om300303a.

[34] A. Begouin, M.-J.R.P. Querioz, Scope and limitations of the base-free copper (I) oxide catalyzed N -heteroarylation of 1H -(Benz) imidazoles with B-heteroarylboronic acids, Helv. Chim. Acta 96 (2013) 853–863, https://doi.org/10.1002/hlca.201200310.

[35] W.W.N. O, A.J. Lough, R.H. Morris, Palladium(II) and platinum(II) complexes featuring a nitrile-functionalized N-heterocyclic carbene ligand, Organometallics 29 (2010) 570–581, https://doi.org/10.1021/om9008372.

[36] O. Ciftci, I. Ozdemir, N. Vardi, N. Gurbuz, Novel platinum- N -heterocyclic carbene complex is more cardiotoxic than cis-platin in rats, Hum. Exp. Toxicol. 30 (2011) 1342–1349, https://doi.org/10.1177/0960327110390064.

[37] N. Godbert, T. Pugliese, I. Aiello, A. Bellusci, A. Crispini, M. Ghedini, Efficient, ultrafast, microwave-assisted syntheses of cycloplatinated complexes, Eur. J. Inorg. Chem. 2007 (2007) 5105–5111, https://doi.org/10.1002/ejic.200700639.

[38] C.M. Anderson, M.A. Weinstein, J. Morris, N. Kfoury, L. Duman, T.A. Balema, A. Kreider-Mueller, P. Scheetz, S. Ferrara, M. Chierchia, J.M. Tanski, Biscyclometalated platinum complexes with thiophene ligands, J. Organomet. Chem. 723 (2013) 188–197, https://doi.org/10.1016/J.JORGANCHEM.2012.10.027.

[39] M. Bachmann, D. Suter, O. Blacque, K. Venkatesan, Tunable and efficient white light phosphorescent emission based on single component N-heterocyclic carbene platinum(II) complexes, Inorg. Chem. 55 (2016) 4733–4745, https://doi.org/10.1021/acs.inorgchem.5b02962.

[40] R.A. Thomas, C.N. Tsai, S. Mazumder, I.C. Lu, R.L. Lord, H.B. Schlegel, Y.J. Chen, J.F. Endicott, Energy dependence of the ruthenium(II)-Bipyridine metal-to-ligand-charge-transfer excited state radiative lifetimes: effects of $\pi\pi^*$(bipyridine) mixing, J. Phys. Chem. B 119 (2015) 7393–7406, https://doi.org/10.1021/jp510949x.

[41] S.S.M. Ling, I.R. Jobe, L. Manojlovic-Muir, K.W. Muir, R.J. Puddephatt, Oxidative addition of methyl iodide to binuclear complexes [$Pt_2Me_4(\mu-R_2PCH_2PR_2)_2$] and the crystal structure of a bridged Pt(IV)-Pt(IV) product, [$Me_3Pt(\mu-I)(\mu-Me_2PCH_2PMe_2)_2PtMe_3$]I, Organometallics 4 (1985) 1198–1202, https://doi.org/10.1021/om00126a011.

[42] Mehdi Rashidi, S. Masoud Nabavizadeh, A. Akbari, S. Habibzadeh, Secondary Kinetic Deuterium Isotope Effects in the Reaction of MeI with Organoplatinum(II) Complexes, 2005, https://doi.org/10.1021/OM0500016.

[43] R.P. Hughes, M.A. Meyer, M.D. Tawa, A.J. Ward, A. Williamson, A.L. Rheingold, L.N. Zakharov, Does A-Fluorination Affect the Structural Trans-Influence and Kinetic Trans-Effect of an Alkyl Ligand? Molecular Structures of Pd(TMEDA)(CH_3)(RF) and a Kinetic Study of the Trans to Cis Isomerization of Pt(TMEDA)(CH_3)₂I(RF) [RF = CF_2CF_3, $CFHCF_3$, CH_2CF_3], 2003, https://doi.org/10.1021/IC030251J.

[44] L. Maidich, A. Zucca, G.J. Clarkson, J.P. Rourke, Oxidative addition of MeI to a rollover complex of platinum(II): isolation of the kinetic product, Organometallics 32 (2013) 3371–3375, https://doi.org/10.1021/om400300n.

[45] K.I. Goldberg, J. Yan, E.M. Breitung, Energetics and mechanisms of carbon-carbon and carbon-iodide reductive elimination from a Pt(IV) center, J. Am. Chem. Soc. 117 (1995) 6889–6896, https://doi.org/10.1021/ja00131a010.

[46] C.J.L, R.J. Puddephatt, Rapid Reversible Oxidative Addition of Group 14–Halide Bonds to Platinum(II): Rates, Equilibria, and Bond Energies, 1997, https://doi.org/10.1021/JA971532R.

[47] E.G. Bowes, S. Pal, J.A. Love, Exclusive csp^3-csp^3 vs csp^2-csp^3 reductive elimination governed by ligand constraints, J. Am. Chem. Soc. 137 (2015) 16004–16007, https://doi.org/10.1021/jacs.5b10993.

[48] K.I. Goldberg, J.Y. Yan, E.L. Winter, Competitive carbon-carbon reductive elimination and carbon-iodide bond formation from a Pt(IV) complex, J. Am. Chem. Soc. 116 (1994) 1573–1574, https://doi.org/10.1021/ja00083a054.

[49] B.J. Coe, M.K. Peers, N.S. Scrutton, Syntheses and electronic and optical properties of complexes of the bis(2,2′-bipyrazyl)ruthenium unit, Polyhedron 96 (2015) 57–65, https://doi.org/10.1016/J.POLY.2015.04.028.

[50] S. Záliš, M. Busby, T. Kotrba, ‖.P. Matousek, M. Towrie, A. Vlček, Excited-state Characters and Dynamics of [W(CO)5(4-cyanopyridine)] and [W(CO)5(piperidine)] Studied by Picosecond Time-resolved IR and Resonance Raman Spectroscopy and DFT Calculations: Roles of W→L and W→CO MLCT and LF Excited States Revised, 2004, https://doi.org/10.1021/IC035089Z.

[51] C.N. Tsai, Y.-H. Tian, X. Shi, R.L. Lord, H.B. Schlegel, Y.J. Chen, J.F. Endicott, Experimental and DFT characterization of metal-to-ligand charge-transfer excited states of (Rutheniumammine)(Monodentate aromatic ligand) chromophores, Inorg. Chem. 52 (2013) 9774–9790, https://doi.org/10.1021/ic4016614.

[52] V.M. Fernández-Alvarez, S.K.Y. Ho, G.J.P. Britovsek, F. Maseras, A DFT-based mechanistic proposal for the light-driven insertion of dioxygen into Pt(ii)–C bonds, Chem. Sci. 9 (2018) 5039–5046, https://doi.org/10.1039/C8SC01161C.

[53] J. Brooks, Y. Babayan, S. Lamansky, P.I. Djurovich, I. Tsyba, R. Bau, M.E. Thompson, Synthesis and Characterization of Phosphorescent Cyclometalated Platinum Complexes, 2002, https://doi.org/10.1021/IC0255508.

[54] V.N. Kozhevnikov, M.C. Durrant, J.A.G. Williams, Highly luminescent mixed-metal Pt(II)/Ir(III) complexes: bis-cyclometalation of 4,6-diphenylpyrimidine as a versatile route to rigid multimetallic assemblies, Inorg. Chem. 50 (2011) 6304–6313, https://doi.org/10.1021/ic200706e.

[55] H. Leopold, T. Strassner, 4,5-Substituted C˄C* cyclometalated thiazol-2-ylidene platinum(ii) complexes − synthesis and photophysical properties, Dalton Trans. 46 (2017) 7800–7812, https://doi.org/10.1039/C7DT00828G.

[56] H. Leopold, U. Heinemeyer, G. Wagenblast, I. Münster, T. Strassner, Changing the emission properties of phosphorescent C˄C*-Cyclometalated thiazol-2-ylidene platinum(II) complexes by variation of the β-diketonate ligands, Chem. Eur. J. 23 (2017) 1118–1128, https://doi.org/10.1002/chem.201604456.

[57] H. Leopold, A. Tronnier, G. Wagenblast, I. Münster, T. Strassner, Photoluminescence of a new material: cyclometalated C˄C* thiazole-2-ylidene platinum(II) complexes, Organometallics 35 (2016) 959–971, https://doi.org/10.1021/acs.organomet.5b00991.

[58] G.M. Sheldrick, A short history of SHELX, Acta Crystallogr. Sect. A Found. Crystallogr. 64 (2008) 112–122, https://doi.org/10.1107/S0108767307043930.